



Numerical evaluation of the effect of using twisted tapes as turbulator with various geometries in both sides of a double-pipe heat exchanger

Mehdi Noorbakhsh¹ · Mohammad Zaboli¹ · Seyed Soheil Mousavi Ajarostaghi²

Received: 10 March 2019 / Accepted: 14 June 2019 / Published online: 26 June 2019
© Akadémiai Kiadó, Budapest, Hungary 2019

Abstract

In this study, the effect of using twisted tapes with various geometries in both tubes of a double-pipe heat exchanger is numerically investigated. The twisted tapes are inserted in both sides of double-pipe heat exchanger to improve the heat transfer where the fluid is water in both sides. The influence of geometrical parameters including the number of twisted tape and creating hollow on twisted tape with different aspect ratios is investigated numerically. The obtained results are analyzed by calculating the outlet temperature of both sides, pressure drop, Nusselt number, and coefficient of performance. Numerical simulations are performed by a commercial CFD code, ANSYS FLUENT 18.2. The results indicate that increasing the number of twisted tape from one-fin to four-fin leads to an increase in the Nusselt number 3.1%, pressure drop 64%, and coefficient of performance 63.9%. Eventually, based on outcomes, four-fin twisted tapes provided better coefficient of performance. In the second part of the study, the effect of creating hollow on the four-fin twisted tape with different aspect ratios ($AR = W/H$) is studied. Three different aspect ratios including 2.25, 1, and 0.44 are considered. The results show that creating the hollows with $AR = 1$ on the twisted tape leads to better coefficient of performance.

Keywords Heat exchanger · Twisted tape · Turbulator · Numerical model

Introduction

The transfer of thermal energy from a fluid to another fluid in the industry is carried out by a double-pipe heat exchanger. There are two fluids with different temperatures in the heat exchanger which provides the condition for exchanging the heat between two fluids. Typically, heat exchangers have been used for cooling the hot fluid or heating the cold fluid, or both. The application of heat exchangers is very wide, and they have used in various industries such as power plants, refineries, food industry,

pharmacy, petrochemical industry, chemical industry, electronics, environmental engineering, space applications, cool stores, heating, and cooling systems for buildings, and in general, wherever the issue of exchanging energy is concerned.

Improvement in heat transfer of heat exchangers has always been one of the most important challenges in industrial and engineering equipment. Researchers have been looking for a way to achieve higher efficiency in heat exchangers. Berger et al. [1] divided heat transfer enhancement methods into two types of active and passive. Passive methods do not need external forces and can be implemented by creating turbulence in flow, changing the heat exchanger geometry, etc. The secondary flow loops were first observed by Eustice [2] which plays an important role in passive methods to improve the coefficient of performance of the considered system.

The double-pipe heat exchangers are made of two concentric tubes in which the start and end of the tubes individually connected to the inlet and outlet of the fluid with different characteristics. According to the company manufacturing heat exchangers, the double-pipe heat

✉ Seyed Soheil Mousavi Ajarostaghi
s.s.mousavi@stu.nit.ac.ir

Mehdi Noorbakhsh
mehdi.noorbakhsh@ustmb.ac.ir

Mohammad Zaboli
mohammad.zaboli@ustmb.ac.ir

¹ Department of Mechanical Engineering, Mazandaran University of Science and Technology, Babol, Iran

² Department of Mechanical Engineering, Babol Noshirvani University of Technology, Babol, Iran

exchangers are suitable for viscosity fluids with low flow rates that need heating and cooling. This type of heat exchangers is composed of two tubes, one in the other. A fluid passes through the smaller tube, and the other fluid moves around it, so heat transfer takes place between two fluids.

One of the most effective passive methods for improving heat transfer is the use of a twisted tape inside the tube that does not require external energy and improves heat transfer by generating rotational fluid flow.

Twisted tapes are widely used in heat exchangers in industrial applications including chemical engineering processes of heat recovery, air conditioning and refrigeration, chemical reactors, power plants, and nuclear reactors due to creating rotational fluid flow and increasing heat transfer as a way for decreasing mass, size, and cost. The secondary flow created by these tapes affects the fluid flowing through the tube and increases the turbulence and heat transfer coefficient. This rotational flow causes turbulence near the tube wall and increases the time of retaining the fluid inside the tube. Numerous studies have been carried out on the use of the twisted tapes to improve heat transfer in heat exchangers. Some of them are as follows.

Kumar and Prasad [3] experimentally investigated utilization of simple twisted tapes. The results showed that the twisted tapes generated turbulence in the fluid inside the tube which resulted in enhancing heat transfer. Reducing the torsion ratio leads to an increase in the heat transfer rate and pressure drop. Jaisankar et al. [4] examined a normal twisted tape. The ratio of Nusselt number of this case to the Nusselt number of a plain tube is 2–2.5, the ratio of the friction coefficient to the friction coefficient of a plain tube is 1.5–2, and the Reynolds number is from 3000 to 23,000. Eiamsa-Ard et al. [5] studied the increase in heat transfer attributed to twisted tapes. The results indicated that the heat transfer rate and friction coefficient increased with decreasing the torsion ratio and spiral pitch. Eiamsa-Ard et al. [6] investigated the twisted tapes with central wings and different axes. The combination of these two led to better mixing of fluid flow and enhancing heat transfer compared to using each one individually. Also, the Nusselt number increases with increase in angle of attack. Eiamsa-Ard and Promvonge [7] examined the twisted tapes in a clockwise and counterclockwise direction. The ratio of Nusselt number of this case to Nusselt number of a normal tape is 12.8–41.9%, and the ratio of the friction coefficient of this case to the friction coefficient of a normal tape is 12.5–41.5%. The Reynolds number is in the range of 3000–27,000. Eiamsa-Ard et al. [8] studied the heat transfer in a pipe with double twisted tapes. The ratio of Nusselt number of this case to the Nusselt number of a

normal tape is 50%, and the Reynolds number is from 3700 to 21,000.

Thianpong et al. [9] studied the hollow twisted tapes. The ratio of the Nusselt number of this case to that of a plain tube is 1.5–2.5. Also, the ratio of the friction coefficient of this case to that of a plain tube is 8–12. Eiamsa-Ard and Promvonge [10] examined the serrated tapes. The ratio of the Nusselt number of this case to that of a plain tube and a tube with a normal tape is 72.2% and 27%, respectively. The ratio of the friction coefficient of this case to that of a plain tube is 2.2, and the Reynolds number is from 4000 to 20,000. Murugesan et al. [11] investigated the square-cut twisted tapes. The ratio of the Nusselt number of this case to that of a tube with a normal tape is 1.14. Also, the ratio of the friction coefficient of this case to that of a tube with a normal tape is 1.25. The Reynolds number is from 2000 to 12,000. The twisted tapes with springy wire were studied by Promvonge [12]. The ratio of the Nusselt number of this case to that of a plain tube is 3–6, and the ratio of the friction coefficient of this case to that of a plain tube is 28–64. The Reynolds number is from 3,000 to 18,000.

Darzi et al. [13] examined numerically the heat transfer in a spiral, wavy tube for pure water and water-containing aluminum oxide nanofluid. The results showed that the utilizing of spiral, wavy tube and water-containing aluminum oxide nanofluid leads to an increase in heat transfer compared with using pure water in a plain tube of about 330%. An investigation of the performance of a modified double-glazed heat exchanger with twisted tapes and rotational flow on both sides was carried out by Shaji [14]. Numerical analysis was conducted for turbulent flow conditions with the twisted tapes. (Torsion ratio was 5 and 3.) Wongcharee and Eiamsa-Ard [15] studied the increase in heat transfer using a copper oxide/water nanofluid in a wrinkled tube with the twisted tapes. The investigations were for three different volumetric concentrations, three different torsion ratios, and for two different arrangements of the rotational direction of the twisted tapes as well as the wrinkled tube in counter and parallel flow for Reynolds numbers from 2400 to 6200. The results indicated that the simultaneous usage of the nanofluid and twisted tapes leads to performing more heat transfer and friction compared with usage of them individually. By increasing the volumetric concentration of the nanofluid and reducing the torsion ratio, the heat transfer rate increases. The utilization of twisted tapes with in wrinkled tube in counterflow created more heat transfer than in a parallel flow.

The proposed geometry in this paper is considered to enhance the heat transfer process in the double-pipe heat exchanger. The proposed geometry creates secondary and swirl flow in the channel which leads to more heat transfer rate between fluids of both sides. Heat transfer

enhancement is the process of increasing the effectiveness of heat exchangers. This can be achieved when the heat transfer power of a given device is increased or when the pressure losses generated by the device are reduced. A variety of techniques can be applied to this effect, including generating strong secondary flows or increasing boundary layer turbulence. On the other hand, the base application of heat transfer enhancement methods is in improving the thermal performance of the heat exchanger which has vast applications in industrials.

Although utilizing twisted tape in order to improve the heat transfer rate in heat exchanger has been investigated in significant number of studies, however, in the present paper, the considered twisted tape is used in both sides of double-pipe heat exchanger with the same twist angle which is the novelty of using this type of passive method. The working fluid for hot and cold sides is water. The present study has two sections. At the first section, the three different geometries of twisted tape including two-fin, three-fin, and four-fin types are investigated numerically. At the second section, the hollow is created on the selected twisted tape from the first section. The effect of aspect ratio of hollow which is the ratio of width of the hollow to the height of the hollow is analyzed, and three different aspect ratios of hollow including 2.25, 1, and 0.44 are considered.

The novelty of the present study

According to the comprehensive literature review performed, few significant studies about the discharge process (melting) in ice-on-coil ice storage system with horizontal coil tube have been published so far. The benefit from using horizontal coil tube instead of straight tube to increase the melting rate was not also considered completely in the previous researches. On the other hand, the melting process in a horizontal shell and coil tube ice storage system has not been studied numerically in the last published studies. Also, in this paper, a comprehensive study is presented by considering the influence of both operational and geometrical parameters numerically.

Methodology and numerical simulation

Model domain

The studied geometry is a double-pipe heat exchanger equipped with three types of twisted tapes in both internal and external tubes. This type of heat exchanger consists of two tubes that one of them is placed inside the other one. The hot fluid flows through the internal tube, and cold fluid flows around it (in the external tube), so heat transfer occurs between two fluids. The 3D schematic of the

considered geometry is shown in Fig. 1a. The geometrical parameters of the investigated domain are shown in Fig. 1b. As shown in Fig. 1a, the considered heat exchanger is counterflow type. The values of constant geometrical parameters are listed in Table 1.

Section one: various geometries of twisted tape

At the first section of study, three different geometries of twisted tape are considered which are illustrated in Fig. 2. The investigated geometries are one-fin, three-fin, and four-fin twisted tape. The twisted tape of inner and outer tube has the same twist angle. The diameter of the twisted tape is equal to diameter of the outer tube.

Section two: various geometries of hollow

According to the obtained results from section one of the article, the four-fin twisted tapes with the highest number of the tape have better coefficient of performance. In the second part of this research, the effect of creating hollows with different geometries on the four-fin twisted tapes has been investigated. The hollows are rectangular and have equal area. Numerical simulations have been performed for different aspect ratios ($AR = W/H$) of the hollows such as 2.25, 1, and 0.44. In Fig. 3, the four-fin twisted tapes with different geometries are illustrated. The values of the geometric parameters of the hollows are given in Table 2.

Considered grid for numerical simulations

Figure 4 shows the considered grid for performing the numerical simulations. As can be seen, it indicates the meshing of the studied double-pipe heat exchanger. In order to improve the quality of the mesh, the boundary layers for both the inlet and outlet sections have been created. The tetrahedron type cell is used for the grid.

Governing equations

There are various methods for modeling turbulent flows. One of the common methods in fluid mechanics is the direct numerical simulation. Due to the long solution process of the turbulent flows and time-consuming nature of the direct method, today's computers are not useful from the point of view of cost and time for this method. In this method, the components of the solution network are too small in which no turbulent model is used. This method is also limited by the need for high computational volume, even for flows with low Reynolds number. On the other hand, due to the desire of different industries to use simpler and cost-effective methods, the utilization of the mentioned method for engineering issues is not currently common.

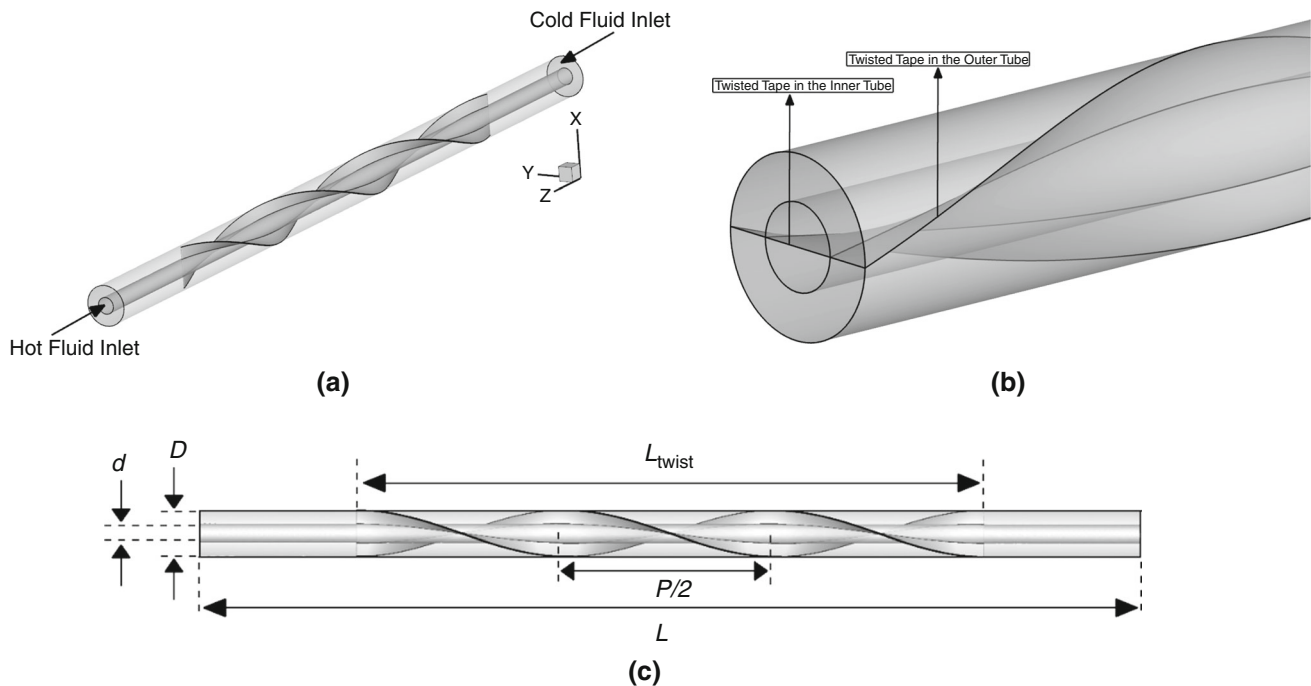


Fig. 1 **a** 3D view of the considered double-pipe heat exchanger, **b** the explanation of the place of the twisted tapes in the heat exchanger, and **c** the geometrical parameters of the considered double-pipe heat exchanger

Table 1 Values of constant geometrical parameters

Parameters		Value (mm)
Length of heat exchanger	L	1200
Length of twisted tape	L_{twist}	800
Diameter of inner tube	d	24
Diameter of outer tube	D	58
Diameter of twisted tape	D	58
Thickness of twisted tape	t	1
Pitch of twisted tape	P	580

Turbulence modeling is the construction and use of a mathematical model to predict the effects of turbulence. In spite of decades of research, there is no analytical theory to predict the evolution of these turbulent flows. The equations governing turbulent flows can only be solved directly for simple cases of flow. For most real-life turbulent flows, CFD simulations use turbulent models to predict the evolution of turbulence. These turbulence models are simplified constitutive equations that predict the statistical evolution of turbulent flows. The Navier–Stokes equations govern the velocity and pressure of a fluid flow. In a turbulent flow, each of these quantities may be decomposed into a mean part and a fluctuating part. Averaging the equations gives the Reynolds-averaged Navier–Stokes (RANS) equations, which govern the mean flow. However,

the nonlinearity of the Navier–Stokes equations means that the velocity fluctuations still appear in the RANS equations, in the nonlinear. This term is known as the Reynolds stress. Its effect on the mean flow is like that of a stress term, such as from pressure or viscosity.

In 1877, Boussinesq proposed relating the turbulence stresses to the mean flow to close the system of equations. Here, the Boussinesq hypothesis is applied to model the Reynolds stress term. Note that a new proportionality constant $\nu_t > 0$ the turbulence eddy viscosity has been introduced. Models of this type are known as eddy viscosity models or EVM's. In this model, the additional turbulence stresses are given by augmenting the molecular viscosity with an eddy viscosity. This can be a simple constant eddy viscosity (which works well for some free shear flows such as axisymmetric jets, 2-D jets, and mixing layers). In general, the eddy viscosity models are divided into three categories of zero-, one-, and two-equation models [16, 17].

The most important difference between the two-equation model and the other models is that they can be used without any prior knowledge of the structure and flow geometry to predict the properties of a turbulent flow. In both the zero-equation model and one-equation model, there is a length of scales in the equations, in which in order to determine its size, there is a need to know the regime and shape of the flow. This makes the simulation of turbulent flows a little complicated before solving it. The two-equation models include standard k – ϵ , RNG k – ϵ ,

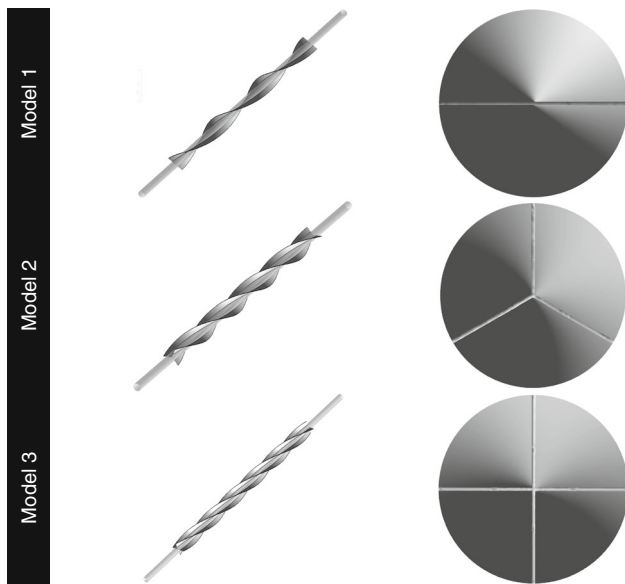


Fig. 2 3D and 2D schematics of the considered twisted tapes for the numerical simulations

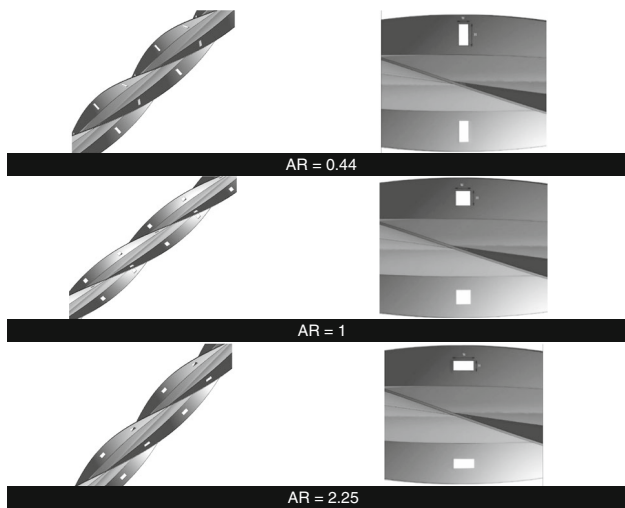


Fig. 3 Schematic of the considered hollow of twisted tapes with different aspect ratios

realizable $k-\epsilon$, standard $k-\omega$, baseline (BSL) $k-\omega$, and shear stress transport (SST) $k-\omega$ models. The turbulence model used in this study is the realizable $k-\omega$ model.

The standard $K-\epsilon$ model has used widely in computational fluid dynamics. This model works well for boundary layer flows and provides acceptable results. But, this model works poorly in the flows with high shear rates or flows with high separation and predicts eddy's viscosity more than its real value. In addition, in these flows, the standard deviation rate equation does not provide a

suitable turbulence length scale. In order to improve the performance of the eddy viscosity $K-\epsilon$ model for predicting complex turbulent flows and eliminating weaknesses and deficiencies, another model is introduced which is called realizable $k-\epsilon$ model. The fundamental differences between the realizable $K-\epsilon$ model and the standard $K-\epsilon$ model are as follows:

- It uses a new formula to calculate the viscosity of turbulence.
- It uses the complete transition equation of mean derived velocity fluctuations to calculate the loss rate of ϵ .

The realizable $K-\epsilon$ model is valid for a wide range of flows such as rotational homogeneous shear flows, free-boundary shear flows, boundary layer flows on a flat plate and inside a channel with and without the pressure gradient, and flows passing through a staircase. In all the flows that are mentioned, the realizable $K-\epsilon$ model is more effective than the standard model. If the flow consists of curved flow lines, virtualization, and extreme rotation, both RNG and realizable $K-\epsilon$ models perform better than the standard model. It should be noted that early studies have shown the realizable $K-\epsilon$ model in complex secondary flows has a high capability compared with the other $K-\epsilon$ models. The governing equations of this problem are presented as follows [16, 17]:

Continuity equation:

$$\frac{\partial(\bar{v}_i)}{\partial x_i} = 0 \tag{1}$$

Momentum equation:

$$\rho \left(\frac{\partial \bar{u}_i}{\partial x_j} + \bar{u}_j \frac{\partial \bar{u}_i}{\partial x_j} \right) = -\frac{\partial \bar{P}}{\partial x_i} + \frac{\partial}{\partial x_j} \left(\mu \frac{\partial \bar{u}_i}{\partial x_j} + \rho \overline{u_i u_j} \right) \tag{2}$$

The transport equations for realizable $k-\epsilon$ model are [16, 17]:

$$\frac{\partial(\rho K)}{\partial t} + \frac{\partial(\rho K v_j)}{\partial t} = \frac{\partial}{\partial t} \left[\left(\mu + \frac{\mu_t}{\sigma_k} \right) \frac{\partial K}{\partial t} \right] + G_k + G_b + \rho \epsilon - Y_M + S_k \tag{3}$$

$$\frac{\partial(\rho \epsilon)}{\partial t} + \frac{\partial(\rho \epsilon v_j)}{\partial t} = \frac{\partial}{\partial t} \left[\left(\mu + \frac{\mu_t}{\sigma_\epsilon} \right) \frac{\partial \epsilon}{\partial t} \right] + \rho C_1 + \rho C_2 \frac{\epsilon^2}{k + \sqrt{v \epsilon}} + C_{1\epsilon} \frac{\epsilon}{k} C_{3\epsilon} G_b + S_\epsilon \tag{4}$$

where

$$C_1 = \max \left(0.43, \frac{\beta}{\beta + 5} \right) \tag{5}$$

Table 2 Values of hollow's geometrical parameters for different AR

Aspect ratio (AR)	Width of hollow (W)/mm	Height of hollow (H)/mm	Area of hollow (A)/mm ²
0.44	4	9	36
1	6	6	36
2.25	9	4	36

$$\beta = S \frac{K}{\epsilon} \quad (6)$$

$$S = \sqrt{2S_{ij}S_{ij}} \quad (7)$$

The first transported Eq. (3) determines the turbulent kinetic energy (k). The second transported Eq. (4) determines the turbulent dissipation (ϵ) which is the rate of dissipation of the turbulent kinetic energy. G_b is generation of turbulence kinetic energy due to buoyancy, G_k is generation of turbulence kinetic energy due to the mean velocity gradients, μ_t is turbulent viscosity of fluid, and S_k and S_ϵ are user defined source terms. Energy equation:

$$\frac{\partial(\rho\bar{T})}{\partial x_i} + \frac{\partial(\rho\bar{u}_i\bar{T})}{\partial x_i} = \frac{\partial}{\partial x_i} \left(\frac{k}{c_p} \frac{\partial(\bar{T})}{\partial x_i} \right) \quad (8)$$

In order to evaluate the results, some parameters including the non-dimensional numbers are necessary that will be as follows:

Reynolds number:

$$Re = \frac{\rho u d_h}{\mu} \quad (9)$$

where d_h is hydraulic diameter of pillow-plate channel that presented by Piper et al. [6] as:

$$d_{h,i} = \frac{4V_i}{A_{wt,i}} \quad (10)$$

where V_i is the volume of a periodic element of the heat exchanger channel, and A_{wt} is the wetted area of the periodic element.

Friction factor (f):

$$f = \frac{2d_h\Delta P}{\rho u^2 L} \quad (11)$$

The coefficient of performance (COP):

Usually, the coefficient of performance (COP) is used to evaluate the performance of the heat exchanger, which shows the effect of improving the heat transfer under known pumping power. This parameter is defined by [18–20]:

$$COP = \left(\frac{Nu}{Nu_0} \right) \left(\frac{f_0}{f} \right)^{\frac{1}{3}} \quad (12)$$

where the Nu_0 and f_0 refer to heat transfer coefficient and friction factor of base model, respectively.

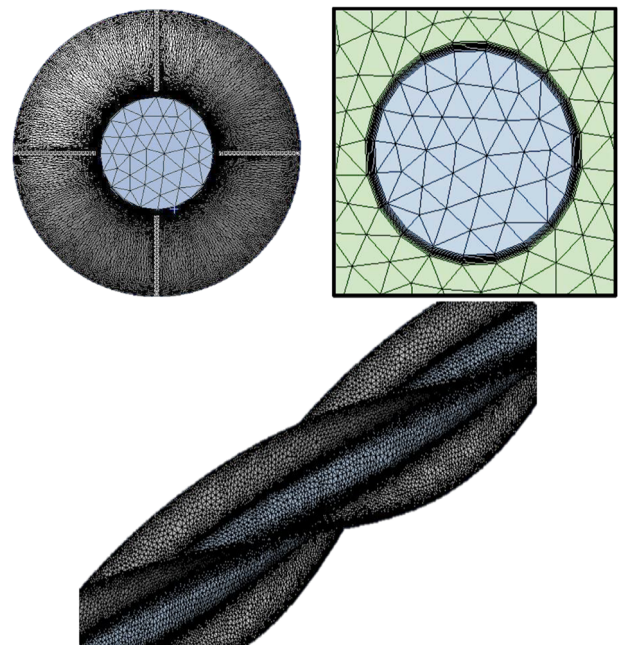


Fig. 4 Generated grid for performing the numerical simulations

Boundary conditions

In the studied heat exchanger, the hot fluid enters into the internal tube at 80 °C with four velocities of 0.14, 0.17, 0.20, and 0.23 m/s, and the cold fluid enters into the external tube at 27 °C and 0.14 m/s. The flow is completely turbulent, and the material of twisted tapes and tubes is aluminum. To clarify the boundary condition of the numerical simulations, the details are listed in Table 3.

Results and discussion

In the present study, the effect of using twisted tape with the same twist angle in both side of double-pipe heat exchanger is studied numerically. The outer diameter of the twisted tape is equal with the diameter of the outer diameter of the heat exchanger. The numerical study is performed in two sections. At the first section of study, three different geometries of the twisted tape including two-fin, three-fin, and four-fin twisted tapes are considered which are shown in Fig. 1 and the values of geometrical

Table 3 Considered boundary conditions for the numerical study

Parameter		Value
Inlet temperature of hot flow (internal tube)/°C	$T_{Inlet, Hot}$	80
Inlet temperature of cold flow (external tube)/°C	$T_{Inlet, Cold}$	27
Inlet velocity of hot flow (internal tube)/m/s	$V_{Inlet, Hot}$	0.14–0.23
Inlet velocity of cold flow (external tube)/m/s	$V_{Inlet, Cold}$	0.14
Reynolds number of hot flow (internal tube)	$Re_{Inlet, Hot}$	3343–5492
Reynolds number of cold flow (external tube)	$Re_{Inlet, Cold}$	3343

parameters are listed in Table 1. At the second section, one of the considered geometries from section one is selected to create hallow on the twisted tape of outer tube to decrease the presser drop in the heat exchanger. Also, three different aspect ratios of created hallow are investigated numerically.

Validation of the present numerical study

To validate the numerical simulation of the present study, the present numerical results are compared with the results of Shaji [14] that are shown in Fig. 5. As can be seen, the percentage error between the present study and the reference results is less than 5%.

The effect of the geometry of utilized twisted tape

In this section, three different twisted tapes as models 1–3 are utilized for performing simulations. The geometries and the values of geometrical parameters are illustrated in

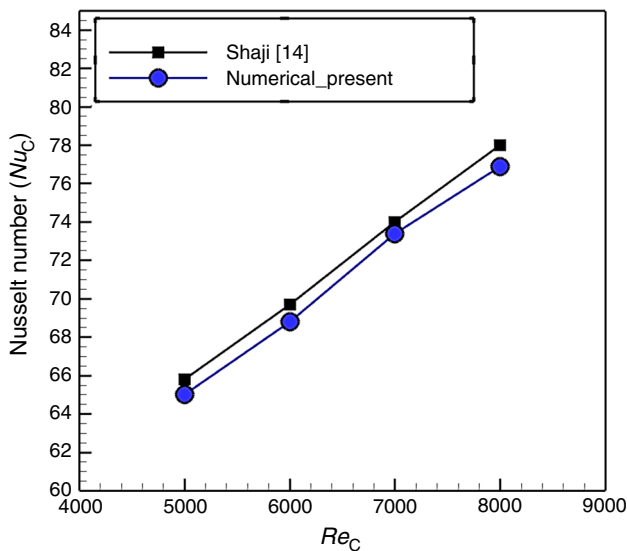


Fig. 5 Nusselt number versus Reynolds number of the cold flow between the present study and the results of Shaji [14]

Fig. 1 and Table 1, respectively. It should be noted that the operational parameters of hot and cold fluid flows are kept constant. In Fig. 6, the outlet temperature of hot and cold fluid flows versus Reynolds numbers for different models is illustrated. The results are obtained for four different Reynolds number between 3343 and 5496.

As shown in Fig. 6a, by increasing the Reynolds number of hot fluid, the outlet temperature of the hot fluid increases as well, since by increase in the Reynolds number, the fluid velocity increases which resulting in decrease in the duration (time period) that the fluid is in contact with the surface of the cold fluid tube. As a result, the much increase in temperature can happen at lower velocities. The outlet temperature of the hot fluid (inside the internal tube) of model 1 for $Re = 4059, 4776,$ and 5496 is 0.7%, 1.4%, and 1.9% higher than that for $Re = 3343$, respectively. The increase in Reynolds number increases the total heat transfer coefficient which is completely justifiable. As shown in Fig. 6a, with increase in the number of twisted tapes from two to four (model 1 to model 3), the outlet temperature of the hot fluid is reduced. The reason for this reduction is the higher number of tapes in model 3 than in models 1 and 2, as by increase in the number of twisted tapes, rotation, and turbulence of the fluid increase significantly. Moreover, naturally due to higher heat transfer in model 3, the heat transfer in this model increases compared to other models which results in a lower outlet temperature of hot fluid and improves heat transfer.

According to Fig. 6b, the variation in the outlet temperature of cold fluid with different Reynolds numbers of hot fluid is illustrated. According to this figure, at higher flow rate or Reynolds number of hot fluid, higher outlet temperature achieved because of having different flow rates in the two fluids. When the hot fluid velocity increases, the heat transfer rate increases as well. This heat transfer in the tube depends on the difference in temperature and flow rate, but the flow rate of the cold flow is constant, and this is the temperature difference that is the main cause of the heat transfer. Therefore, by increasing the velocity of the hot fluid, the cold fluid outlet temperature (inside the external tube) is higher than at the lower velocities. The cold fluid outlet temperature in model 1 for

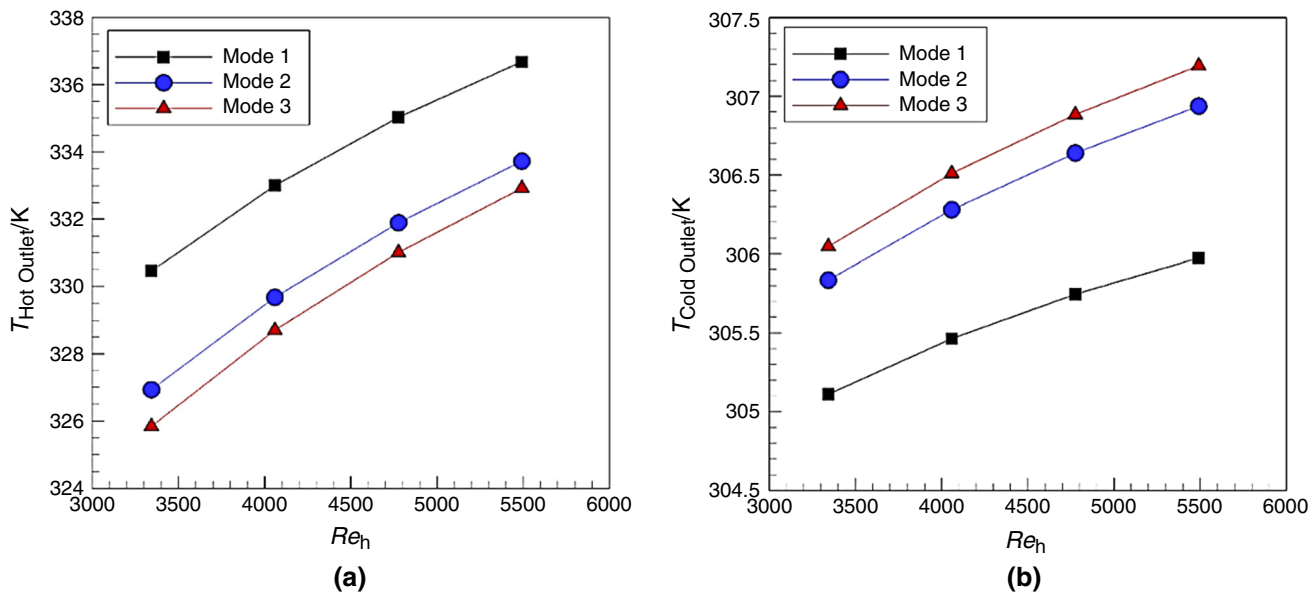


Fig. 6 a Outlet temperature of hot flow versus Reynolds numbers of hot flow for different models. b Outlet temperature of cold flow versus Reynolds numbers of hot flow for different models

$Re = 4059, 4776, \text{ and } 5496$ is $0.1\%, 0.3\%, \text{ and } 0.5\%$ higher than $Re = 3343$, respectively. As shown in Fig. 6b, by increasing the number of twisted tapes from two to four (model 1–3), the cold fluid outlet temperature increases, which is because of the less number of twisted tapes of model 1 than models 2 and 3, as by decreasing the number of twisted tapes the heat transfer area is reduced which leads to increase in the cold fluid outlet temperature of model 3 compared to the other models.

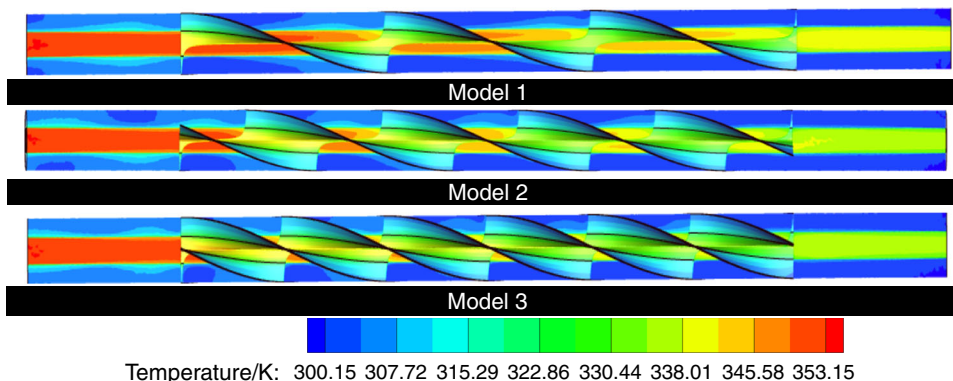
To understand better the heat transfer in different models, in Fig. 7, 2D contours of temperature, and in Fig. 8, 3D contours of the temperature for the hot and cold fluids with different twisted tape geometries are demonstrated. As shown in Figs. 7 and 8, by increasing the fin number of twisted tapes (from model 1 to 3), the fluid rotation between the tube and twisted tape increases, which causes more contact of the fluid flow with the tube wall and twisted tapes and results in providing more heat transfer

rate in the model 3 compared to models 1 and 2. This issue also results in the highest hot fluid outlet temperature in model 1 and the highest cold fluid outlet temperature in model 3. The variation in hot fluid pressure drop with different Reynolds numbers of hot fluid is shown in Fig. 9.

As can be seen in Fig. 9, by increasing the number of twisted tapes from two to four, pressure drop increases. The reason is that by increasing barriers which are the twisted tapes more friction surface and greater involvement between the fluid and the tapes are provided in model 3 compared to models 1 and 2 which leads to increase in pressure drop. According to this figure, at the Reynolds number of 5500, the pressure drop of model 3 is increased by 39% compared to model 1. The variation in the Nusselt number with different Reynolds numbers of hot fluid is illustrated in Fig. 10.

As shown in Fig. 10, the Nusselt number is increased by increasing the Reynolds number. With increase in the

Fig. 7 2D contours of temperature at $Y = 0$ for different models



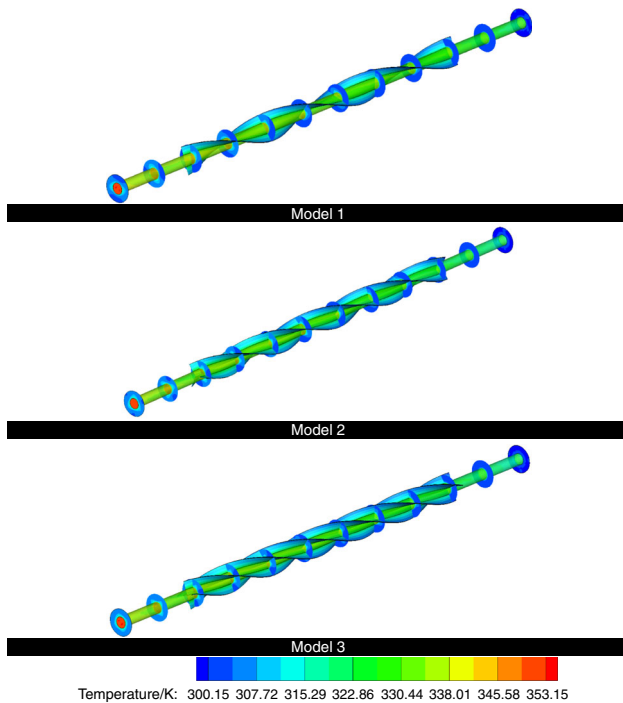


Fig. 8 3D contours of temperature at different slices in the channel for all models

Reynolds number, velocity increases and with this increase, the Nusselt number of model 3 is higher than that of models 1 and 2. The reason is the increase in the number of twisted tapes and turbulence of the fluid in model 3. The Nusselt number in model 1 for the second to fourth velocities is 10.5%, 21%, and 29.8% higher than that for

the first velocity, respectively. Therefore, due to the higher heat transfer area of model 3, heat transfer rate is increased compared to other models, and this causes the higher Nusselt number of model 3 compared to models 1 and 2. Figure 11 shows the variation in the friction coefficient with different Reynolds numbers of hot fluid.

As shown in Fig. 11, by increasing the Reynolds number of the hot fluid, the friction factor decreases too, as by increasing the Reynolds number, the velocity of the fluid increases and based on Eq. (11), the velocity and the friction factor have an inverse relation. Therefore, by increasing the velocity, the friction factor is greater at lower velocities. In Fig. 11, it can be seen that the increase in the friction factor in heat exchangers with more twisted tapes is higher than that in cases with few twisted tapes. The reason is the higher contact area, in other words, the higher friction of model 3 in comparison with models 1 and 2. Thus, the higher the friction and interaction between the fluid and the twisted tapes, the higher the pressure drop, which results in a higher friction factor in model 3 compared to the other models. Figure 12 shows the variation in the coefficient of performance (COP) with different Reynolds numbers of hot fluid.

As shown in Fig. 12, the variation in the coefficient of performance with the changes in hot fluid Reynolds number is illustrated. According to Eq. (12), the coefficient of performance is the ratio of the dimensional Nusselt number and the pressure drop. As shown, for model 3 and the last Reynolds number, the highest coefficient of performance is obtained, which indicates the highest heat transfer rate and the lowest pressure drop.

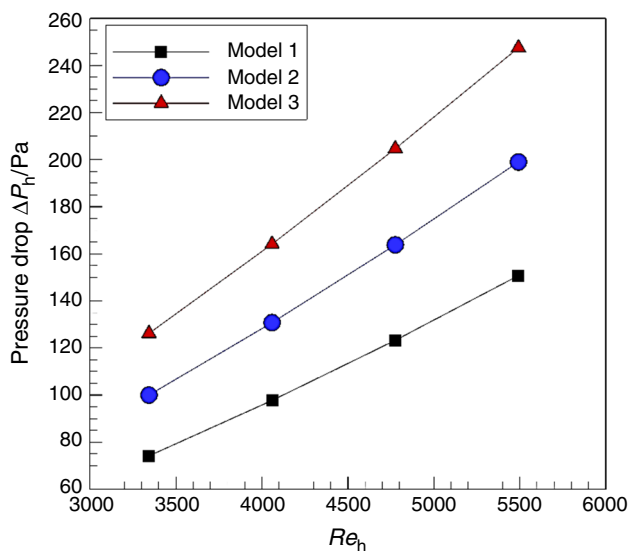


Fig. 9 Pressure drop of hot flow versus Reynolds numbers of hot flow for different models

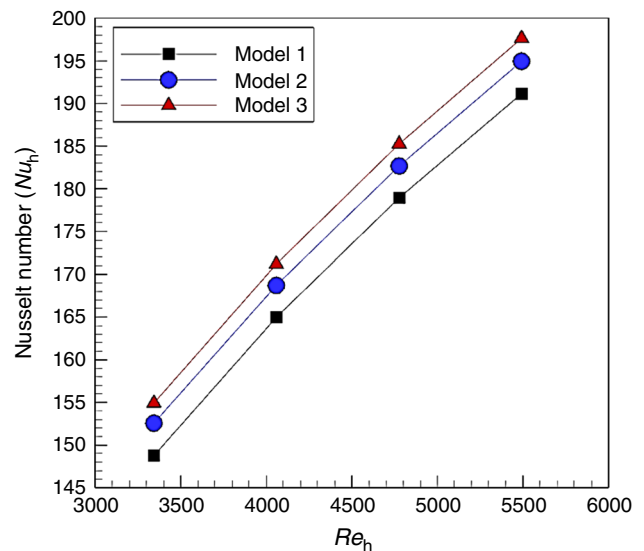


Fig. 10 Nusselt number of hot flow versus Reynolds numbers of hot flow for different models

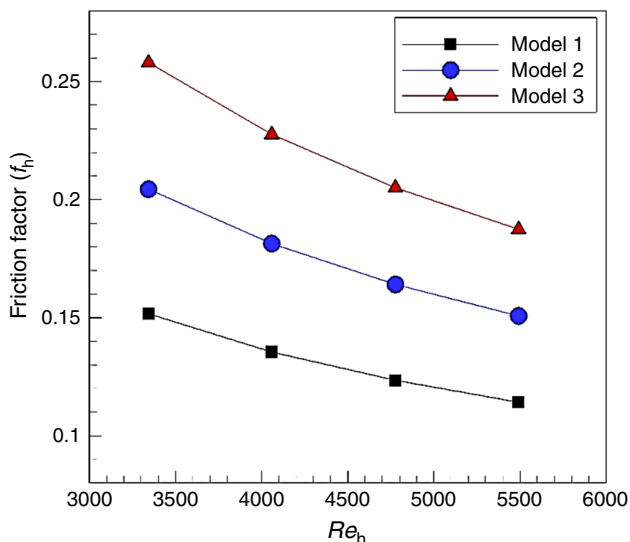


Fig. 11 Friction coefficient of hot flow versus Reynolds numbers of hot flow for different models

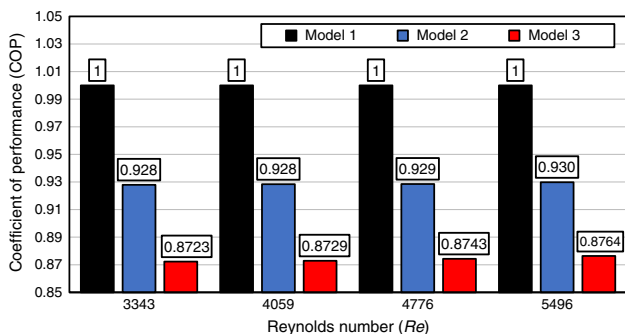


Fig. 12 Coefficient of performance (COP) of hot flow versus Reynolds numbers of hot flow for different models

The effect of the geometry of hole on the selected twisted tape

Because of the best obtained Nusselt number and high pressure drop, model 3 is chosen as the selected model among the others to create holes on its surfaces. Figure 13 demonstrates the variation in the hot fluid outlet temperature of model 3 for various geometries of hollow at different Reynolds numbers of hot fluid.

As illustrated in Fig. 13, according to the comparison between the three models 1–3, with the increase in the Reynolds number of the hot fluid, the outlet temperature of the hot fluid is increased too. Since as the Reynolds number increases, the velocity increases which leads to decreasing the duration in which fluid is in contact with the cold tube surface. This causes an increase in temperature at lower velocities and, in general, an increase in the total heat transfer rate. Based on Fig. 13, in comparing model 3 with

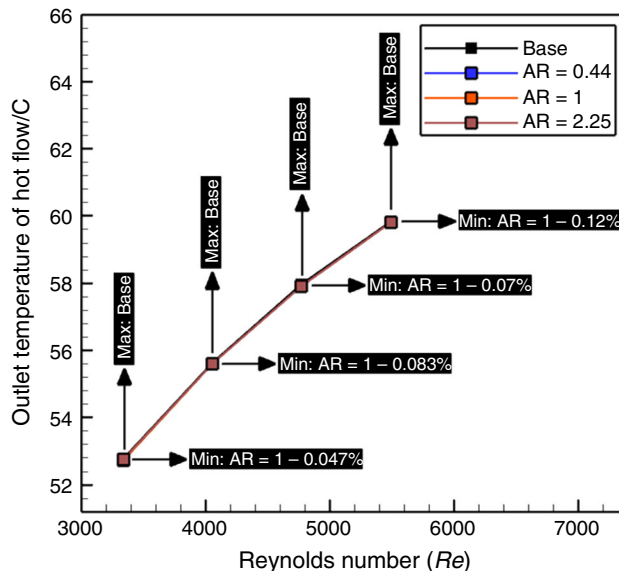


Fig. 13 Outlet temperature of hot flow versus Reynolds number for different AR

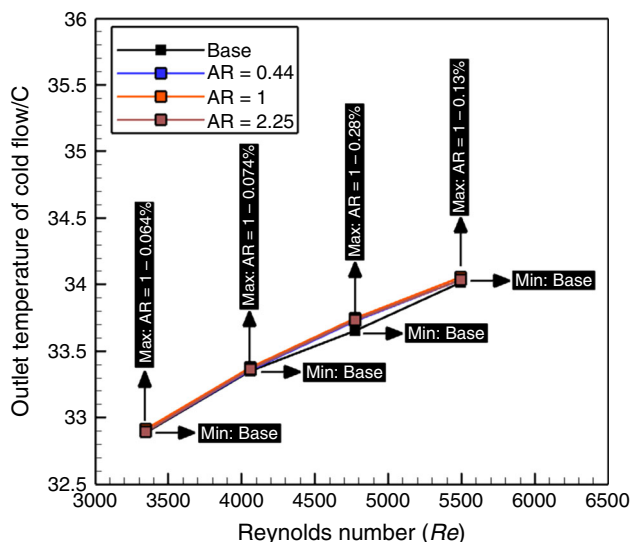


Fig. 14 Outlet temperature of cold flow versus Reynolds number for different AR

hollows at different AR, at first, the proximity in the outlet temperatures and the fewer changes in the outlet temperature of the hot fluid should be considered. However, the non-hollow model has the highest outlet temperature, and model 2 with AR = 1 has the lowest outlet temperature of the hot fluid. Figure 13 indicates the variation in the cold fluid outlet temperature of model 3 with various geometries of hollows at different Reynolds numbers of hot fluid.

Figure 14 shows the variation in the cold fluid outlet temperature of model 3 with various geometries of hollows at different Reynolds numbers of hot fluid. According to this figure, the higher the flow rate or the Reynolds number

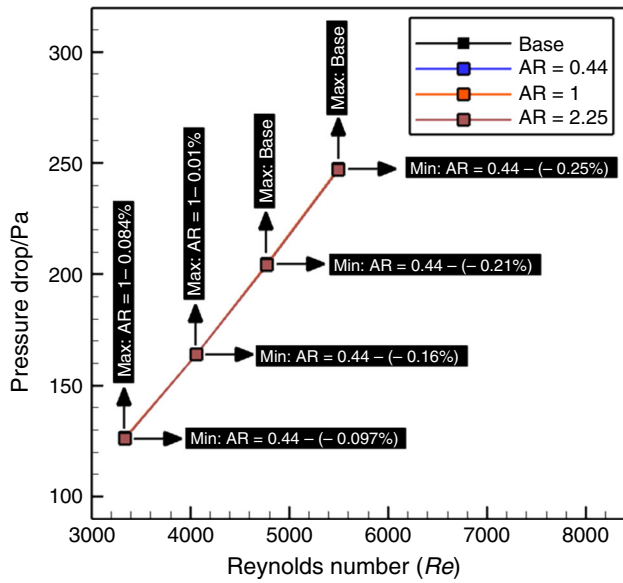


Fig. 15 Pressure drop versus Reynolds number for different AR

of hot fluid, the higher the cold fluid outlet temperature. The reason is different flow rates of the two fluids. When the velocity of the hot fluid increases, it results in an increase in heat transfer rate, which depends on the difference in temperature and flow rate of the hot and cold fluids. It is worth mentioning that flow rate in cold fluid is constant. In fact, the difference in temperature is the main cause of heat transfer. Therefore, with increasing the velocity of the hot fluid, the cold fluid outlet temperature increases at lower velocities. Based on Fig. 14, the temperature difference in outlet temperatures of the cold fluid of model 3 with hollows at different AR is very minor as well as the temperature difference in outlet temperatures of the hot fluid. However, the non-hollow model has the lowest cold fluid outlet temperature and model 2 with AR = 1 has the highest cold fluid outlet temperature. Figure 15 illustrates the variation in the pressure drop of model 3 with various geometries of hollows at different Reynolds numbers of hot fluid.

As shown in Fig. 15, the pressure drop increases with increase in the Reynolds number of the hot fluid. According to this figure, comparing model 3 with hollows at different AR, we can see the proximity of the pressure drop values. However, the model with AR = 0.44 has the lowest pressure drop and the model with AR = 1 has the highest pressure drop. Figure 16 demonstrates the variation in the Nusselt number of model 3 with various geometries of hollows at different Reynolds numbers of hot fluid.

As shown in Fig. 16, increasing the Reynolds number of hot fluid increases the Nusselt number as well. According to this figure, comparing model 3 with hollows at various AR, like the previous figures, indicates that Nusselt

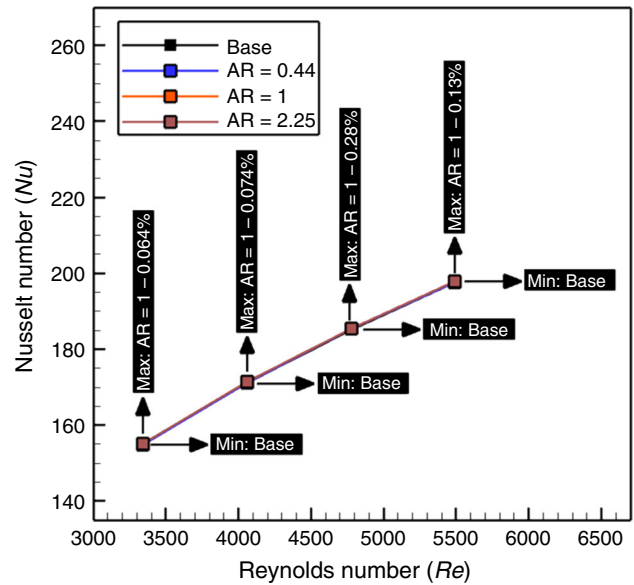


Fig. 16 Average Nusselt number versus Reynolds number for different AR

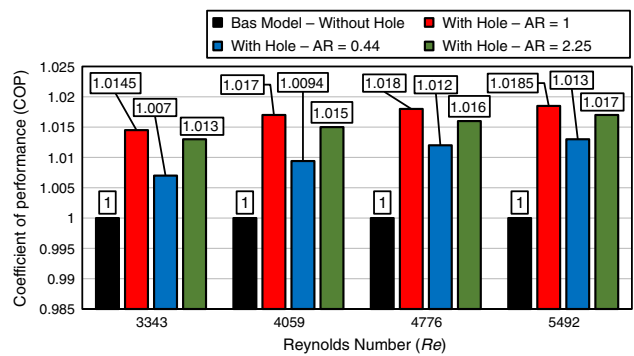


Fig. 17 Coefficient of performance (COP) versus Reynolds number for different AR

numbers in various geometries of hollows are very close to that in the non-hollow model. However, the non-hollow model has the lowest Nusselt number and the model with AR = 1 has the highest one.

The results indicate that hollows with AR = 1 in the twisted tapes improve the Nusselt number and also increase the pressure drop. However, generally, the difference between the twisted tape with and without hollow is not significant. On the other hand, the enhancement of coefficient of performance in creating hollow on the twisted tape in comparison with the twisted tape without hollow is less than 0.1%. The coefficient of performance of the models studied in this section is illustrated in Fig. 17. Accordingly, it can be seen that the differences between the models are very low. However, model with hollow (AR = 1) has more COP (with so small difference) than the other investigated models.

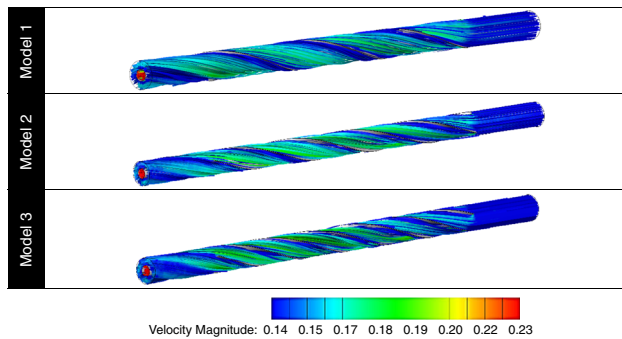


Fig. 18 Streamline with contour of velocity magnitude for different models

According to Fig. 17, it can be realized that at low Re number ($Re = 3343$), model with holes with $AR = 1$ has 1.45% more COP than the base case (without holes) and model with holes with $AR = 0.44$ has 1.3% more COP than base case. On the other hand, creating holes on twisted tape leads to higher COP with various AR . However, holes with $AR = 1$ have the most improvement (with low difference). At high Re number ($Re = 5492$), case with holes with $AR = 0.44$ has 1.3% higher COP and case with holes with $AR = 1$ has 1.85% COP more than base case.

To show the effect of utilizing different types of twisted tape on heat transfer and fluid flow, the streamline with contour of velocity magnitude is illustrated in Fig. 18. It is shown clearly that creating swirl and secondary flows in model 3 of twisted tape because of the number of blade (four) is more than the other investigated models which leads to higher heat transfer rate and model 2 (with three blades) is placed at the second level. As a result, it can be said that utilizing turbulators especially twisted ones has significant effect on creating swirl flow (which leads to higher heat transfer rate) and utilizing twisted tape in both sides of a double-pipe heat exchanger shows better thermal performance and proofed the effect of twisted tape as turbulator on thermal improvement of a double-pipe heat exchanger.

Conclusions

In this study, the effect of using twisted tapes in both tubes of a double-pipe heat exchanger was numerically investigated. The study consists of two sections. At the first section, three different shapes of twisted tape were considered and numerical simulations were performed. At the second step, one of the tested models from section one was selected to create hallow. Three different aspect ratios of hallow were studied. The obtained results consist of outlet temperature, pressure drop, Nusselt number, and

coefficient of performance. The most important outputs are described below.

- In three-fin and four-fin twisted tapes in comparison with two-fin model, the outlet temperature of hot fluid is reduced 1.2% and 1.4%, respectively.
- In three-fin and four-fin twisted tapes in comparison with two-fin model, the outlet temperature of cold fluid in both models is increased less than 1%.
- In three-fin and four-fin twisted tapes in comparison with two-fin model, the pressure drop of hot flow is increased 32% and 64%, respectively.
- In three-fin and four-fin twisted tapes in comparison with two-fin model, the Nusselt number of the hot flow is increased 1.9% and 3.1%, respectively.
- In three-fin and four-fin twisted tapes in comparison with two-fin model, the coefficient of performance of hot flow is increased 31.8% and 63.9%, respectively.
- The results show that creating the hollows with $AR = 1$ on the twisted tape leads to higher coefficient of performance.

References

1. Berger SA, Talbot L, Yao LS. Flow in curved pipes. *Annu Rev Fluid Mech.* 1983;15(1):461–512.
2. Eustice J. Experiments on stream-line motion in curved pipes. *Proc R Soc Lond Ser A.* 1911;85(576):119–31.
3. Kumar A, Prasad BN. Investigation of twisted tape inserted solar water heaters—heat transfer, friction factor and thermal performance results. *Renew Energy.* 2000;19(3):379–98.
4. Jaisankar S, Radhakrishnan TK, Sheeba KN. Experimental studies on heat transfer and friction factor characteristics of thermosyphon solar water heater system fitted with spacer at the trailing edge of twisted tapes. *Appl Therm Eng.* 2009;29(5–6):1224–31.
5. Eiamsa-Ard S, Yongsiri K, Nanan K, Thianpong C. Heat transfer augmentation by helically twisted tapes as swirl and turbulence promoters. *Chem Eng Process.* 2012;60:42–8.
6. Eiamsa-Ard S, Wongcharee K, Eiamsa-Ard P, Thianpong C. Thermohydraulic investigation of turbulent flow through a round tube equipped with twisted tapes consisting of centre wings and alternate-axes. *Exp Thermal Fluid Sci.* 2010;34(8):1151–61.
7. Eiamsa-Ard S, Promvong P. Performance assessment in a heat exchanger tube with alternate clockwise and counter-clockwise twisted-tape inserts. *Int J Heat Mass Transf.* 2010;53(7–8):1364–72.
8. Eiamsa-Ard S, Thianpong C, Eiamsa-Ard P. Turbulent heat transfer enhancement by counter/co-swirling flow in a tube fitted with twin twisted tapes. *Exp Thermal Fluid Sci.* 2010;34(1):53–62.
9. Thianpong C, Eiamsa-Ard P, Promvong P, Eiamsa-Ard S. Effect of perforated twisted-tapes with parallel wings on heat transfer enhancement in a heat exchanger tube. *Energy Procedia.* 2012;14:1117–23.
10. Eiamsa-Ard S, Promvong P. Thermal characteristics in round tube fitted with serrated twisted tape. *Appl Therm Eng.* 2010;30(13):1673–82.

11. Murugesan P, Mayilsamy K, Suresh S. Turbulent heat transfer and pressure drop in tube fitted with square-cut twisted tape. *Chin J Chem Eng.* 2010;18(4):609–17.
12. Promvong P. Thermal augmentation in circular tube with twisted tape and wire coil turbulators. *Energy Convers Manag.* 2008;49(11):2949–55.
13. Darzi AR, Farhadi M, Sedighi K, Aallahyari S, Delavar MA. Turbulent heat transfer of Al_2O_3 –water nanofluid inside helically corrugated tubes: numerical study. *Int Commun Heat Mass Transf.* 2013;41:68–75.
14. Shaji K. Numerical analysis on a double pipe heat exchanger with twisted tape induced swirl flow on both sides. *Procedia Technol.* 2016;24:436–43.
15. Wongcharee K, Eiamsa-Ard S. Heat transfer enhancement by using CuO/water nanofluid in corrugated tube equipped with twisted tape. *Int Commun Heat Mass Transf.* 2012;39(2):251–7.
16. Menter FR. Two-equation eddy-viscosity turbulence models for engineering applications. *AIAA J.* 1994;32(8):1598–605.
17. Wilcox David C. *Turbulence modeling for CFD*, vol. 2. La Canada: DCW industries; 1998.
18. Baragh S, Shokouhmand H, Ajarostaghi SS, Nikian M. An experimental investigation on forced convection heat transfer of single-phase flow in a channel with different arrangements of porous media. *Int J Therm Sci.* 2018;1(134):370–9.
19. Shirzad M, Ajarostaghi SS, Delavar MA, Sedighi K. Improve the thermal performance of the pillow plate heat exchanger by using nanofluid: numerical simulation. *Adv Powder Technol.* 2019;30(7):1356–65.
20. Baragh S, Shokouhmand H, Ajarostaghi SS. Experiments on mist flow and heat transfer in a tube fitted with porous media. *Int J Therm Sci.* 2019;1(137):388–98.

Publisher's Note Springer Nature remains neutral with regard to jurisdictional claims in published maps and institutional affiliations.